Lunar eclipse photometry: absolute luminance measurements and modeling

Nina Hernitschek,[1] Elmar Schmidt,[2,*] and Michael Vollmer[3]

[1]Starkenburg Observatory, Niemöllerstr. 9, 64646 Heppenheim, Germany

[2]SRH University of Applied Sciences, Bonhoefferstrasse 11, 69123 Heidelberg, Germany

[3]Brandenburg University of Applied Sciences, Magdeburger Strasse 50, 14770 Brandenburg, Germany

*Corresponding author: elmar5@web.de

Received 29 April 2008; accepted 13 July 2008;
posted 29 July 2008 (Doc. ID 95632); published 29 August 2008

The Moon's time-dependent luminance was determined during the 9 February 1990 and 3 March 2007 total lunar eclipses by using calibrated, industry standard photometers. After the results were corrected to unit air mass and to standard distances for both Moon and Sun, an absolute calibration was accomplished by using the Sun's known luminance and a pre-eclipse lunar albedo of approximately 13.5%. The measured minimum level of brightness in the total phase of both eclipses was relatively high, namely $-3.32\,m_{vis}$ and $-1.7\,m_{vis}$, which hints at the absence of pronounced stratospheric aerosol. The light curves were modeled in such a way as to let the Moon move through an artificial Earth shadow composed of a multitude of disk and ring zones, containing a relative luminance data set from an atmospheric radiative transfer calculation.

OCIS codes: 010.1290, 010.1285, 010.1310, 010.1320.

1. Introduction

Total lunar eclipses, in which the full Moon's brightness is diminished to a reddish glow for a few hours, were once regarded as signs of godly doom or admonition [1]. The recording of lunar eclipses since ancient times helped resolve the geometry and kinematics of the Sun–Earth–Moon system, so that accurate predictions of solar and lunar eclipses are available today [2]. In more recent times, the photometry of lunar eclipses led to important findings in the atmospheric sciences, because the residual light of the totally eclipsed Moon is sensitive to the refractive, absorptive, and scattering properties of the Earth's atmosphere [3]. Absolutely calibrated measurements, however, have rarely been accomplished, which is to be amended by this study.

0003-6935/08/340H62-10$15.00/0

2. Absolute Luminance Model for the Nearly Full Moon

To present visual brightness variations during total lunar eclipses, the standard photometric quantities are used, because they match the spectral characteristics of the human eye [4].

The nearly full Moon is modeled as a diffuse reflector that is illuminated by the Sun from a distance d. Whereas the disk-averaged (terrestrial) luminance L_s of the Sun is geometrically invariant [5], the solar illuminance E_s depends on both the distance to the Sun as well as to the projection angle of the detector. After the relevant integrations are perfomed, a useful relationship can be established that relates E_s to L_s in the form of the so-called photometric factor [6]

$$\frac{E_s}{L_s} = \Omega_s \left(1 - \frac{\Omega_s}{4\pi}\right) \cos\theta, \tag{1}$$

where Ω_s is the apparent solid angle of the Sun. As seen from the Earth–Moon system, Ω_s is very small compared with 4π, and the angle of incidence is near normal ($\theta \approx 0$), so that expression (1) specializes to

$$E_s = L_s \Omega_s, \tag{2}$$

which presents the maximum direct (i.e., not containing the blue sky luminance) terrestrial component of the solar illuminance (we calculated $E_s \approx 105,000$ lux, based on Eq. (2) with published values for L_s of 1.5×10^9 to 1.6×10^9 cd/m^2[7,8]). Using the average lunar visual albedo C, the Moon's photometric emittance assumes the value $M_m = CE_s$, and its average luminance L_m follows as

$$L_m = \frac{M_m}{\pi} = \frac{1}{\pi} C L_s \Omega_s = C L_s \left(\frac{R_s}{d}\right)^2. \tag{3}$$

Note that d in Eq. (3) is the Moon's, not the Earth's, mean distance from the Sun, and that R_s is the solar radius. The so-called Lambert factor $(1/\pi)$ in Eq. (3) takes into consideration that luminance measurements are calibrated to flat diffuse light sources [5]. The use of only the solar–terrestrial component L_s for obtaining the Moon's terrestrial luminance from Eq. (3) is justified, because although the Moon is of course exposed to the Sun's free-space illumination, its reflected light then penetrates the Earth's atmosphere in almost exactly the same way as sunlight at the respective geometry (with the same relative parts being scattered from the direct beam to brighten the moonlit night sky).

The Moon's direct luminance data reported in Section 4 of this paper were taken in or near lunar eclipses, when earthlight influences are negligible, because the Earth's face visible from the Moon is then not illuminated by the Sun. However, the Moon's albedo C is rapidly changing for dates around the full Moon, when the lunar phase angle ϕ, which is the angle at the Moon vertex of the Sun–Moon–Earth triangle, becomes quite small. A visual albedo of $C = (16.0 \pm 0.1)\%$ has been deduced for $\phi = 0°$ from observations of the lunar orbiter Clementine [9]. The smallest phase angle that the Moon can attain before entering an eclipse is $\phi \approx 1.5°$, for which the same space-based integral brightness measurements yield albedo values of 13.5% [9]. By using the published range in $L_s = 1.5$–1.6×10^9 cd/m^2 for the Sun [7,8], $R_s = 696,000$ km, and $d = 150 \times 10^6$ km[10] for Eq. (3), the mean luminance of the full Moon just outside an eclipse is expected to reach (4500 ± 150) cd/m^2. This value is corroborated by the absolute luminance determinations reported in Section 4. By the same argument a typical full Moon near the phase angle $\phi = 5°$ attains the albedo $C = 11\%$ and a luminance near (3670 ± 120) cd/m^2. These figures have been derived on the basis of photometric principles and space-based reflectance measurements; hence they are believed to be more reliable than other published and public domain values for the full Moon's luminance, which vary between 2500 cd/m^2 [11] and 4200 cd/m^2 [12].

3. Instrumental Errors and Data Reduction

Industrial standard lightmeters, i.e. a Minolta CS-100 and a Minolta LS-110 (nowadays produced by Konica-Minolta) were used for luminance recording during two total lunar eclipses in 1990 and 2007. Both instruments use calibrated silicon photodiodes with a daylight vision $V(\lambda)$ filter and thus are sensitive only to wavelengths in the range of 380–780 nm. Imaging optics restricts the accepted light cone to circular apertures of 1° and $(1/3)°$ across, respectively. Their measurement ranges extend over7–8 orders of magnitude, ranging from 0.01 to 199,000 cd/m^2 (for CS-100) and from 0.01 to 999,000 cd/m^2 (LS-110) [13], which is well suited to the Moon's 4–5 order of magnitude drop of luminance during total eclipses.

The instruments were mounted on heavy-duty photo tripods, pointed at the Moon, and manually triggered at the SLOW response time of 0.4 s. Their absolute accuracy being stated as $\pm 2\%$ implies that the geometrical effects related to the Moon's size and topography are expected to be the dominant source of error in the measurements.

The CS-100's aperture will always detect light from the Moon as seen from the Earth as well as from the surrounding sky. Therefore the instrument does not read true luminance values, but rather values Y_m, which are means of the lunar and dark sky luminances weighted by the respective solid angles. Because the latter is negligible (typically much less than 1 cd/m^2 even under full Moon lighting), this can be compensated for by correcting Y_m with the inverse of the relative solid angle of the Moon within the measuring aperture according to

$$L_m = Y_m \left(\Delta / 2\rho_m\right)^2. \tag{4}$$

Here, Δ is the nominal angular diameter of the CS-100's aperture (60 arc min) and $2\rho_m$ the apparent angular diameter of the Moon. For the latter, we took care to use the diurnally varying topocentric values, obtained from personal computer planetarium software [14], because a correction based on geocentric values could differ by up to 3%. Whether the CS-100's field diameter meets the specified value $\Delta = 60'$ exactly cannot be easily checked directly; therefore full Moon measurements with both instruments were used for a comparison (see Section 4).

In the case of the LS-110's $(1/3)°$ field of measurement, only part of the Moon surface is used for the measurement. Hence, although the instrument readings are in true luminances, they represent only a good 40% of the full Moon's apparent disk. On the other hand, a smaller field of view is an advantage for probing the Earth's shadow during lunar eclipses. The most important experimental concern in using the LS-110 was to diligently center its aperture on the lunar disk, in order not to include varying parts of the lunar topography. Misaligning the instrument intentionally led to a misreading of up to 5%. We

estimate the overall errors in the luminance values from the LS-110 to be typically of the order of ±5%.

The LS-110's absolute calibration was compared with a secondary luminance standard of type LN3, made by LMT Lichtmesstechnik in Berlin, Germany, in a photometric laboratory in Karlsruhe, Germany. The standard had been freshly registered by the manufacturer at values of 1058 cd/m^2 and 108.8 cd/m^2, which also happen to occur during lunar eclipses. The LS-110's readings were lower by only 0.8%, so the lunar luminance values taken in the 2007 eclipse were not affected much by decalibration. Although there is a known difference in the amount of 0.22% between the German and Japanese candela standards [15], which could be subtracted from the 0.8%, we decided to correct the data upward by the full 0.8%, because even this maximum linear effect translates logarithmically into only a hundredth of an astronomical brightness magnitude at the full Moon's luminance.

The Moon's measured luminance is reduced by atmospheric absorption and scattering processes (their combined effect giving rise to an extinction cross section σ_e) according to the varying optical air mass M along the line of sight. An empirical formula by Kasten and Young [16] is used for the dependence of relative air mass on the Moon's zenith angle Z. The small reduction of air mass for the near-sea-level observing altitudes z during the two reported eclipses (cf. Table 1) can be multiplied into this formula by the barometric equation, using $z_0 \approx 8000$ m as the scale height. The resulting expression thus gives a relative value of $M \approx 1$ for $z = 0$ m and $Z = 0°$:

$$M(z,Z) = \frac{\exp(-z/z_0)}{\cos Z + 0.50752 \times (96.07995° - Z)^{-1.6364}}. \quad (5)$$

Table 1. Main Parameters for the Measured Total Lunar Eclipses[a]

Geocentric Eclipse Parameters	Symbol	9 Feb. 1990	3 March 2007
Earth's penumbral radius	ρ_P	74.7 arc min	72.1 arc min
Earth's umbral radius	ρ_U	41.63 arc min	39.21 arc min
Lunar radius at mid eclipse	ρ_m	15.525 arc min	14.855 arc min
Smallest phase angle	$\varphi_{\min}$	23.63 arc min	17.30 arc min
Greatest umbral magnitude	$U_{\max}$	1.0797	1.2375
Time of greatest eclipse		19:11:05 UT	23:20:56 UT
Observation site		Mannheim, Germany	Heppenheim, Germany
Altitude	z	95 m	256 m
Geographical latitude		49° 27′	49°39′
Geographical longitude		8°28′	8°39′

[a]For details and the time lines see [2]].

The luminous flux from an astronomical object is weakened in accordance with the Bouguer–Lambert–Beer law of extinction, provided the optical thickness $\tau(\lambda) = \int n\sigma_e(\lambda)ds$ for the respective path length is known [17]. In general the optical thickness integral will include contributions from both the molecular and the aerosol content. As the latter is usually not known well enough, any terrestrial precision photometry of astronomical objects requires very clear air conditions, when Rayleigh or molecular scattering with $\tau_{\mathrm{Mol}}(\lambda) = Nk_{\mathrm{Mol}}/\lambda^4$ is the only factor of extinction, where N is the total particle number and k_{Mol} the molecular scattering amplitude. As N is proportional to the optical air mass, the following reduction in spectral luminance of the Moon can be expected relative to unit air mass, since the luminances L_s and L_m in Eq. (3) refer to $M = 1$:

$$F(Z,z,\lambda) = \exp\{-\tau_{\mathrm{Mol}}(\lambda)[M(Z,z) - 1)]\}. \quad (6)$$

All lunar luminance data were corrected by the inverse of Eq. (6) by using a mean value $\tau_0 \approx 0.098$, obtained by numerically convoluting the (λ^{-4}) wavelength dependence with the detectors' $V(\lambda)$ characteristics.

The brightness B of astronomical objects like the Moon is usually given in visual magnitudes m_{vis}. These are calculated by comparing the luminous intensity (luminosity) of the respective object to that of certain reference stars of defined luminosity and brightness and then taking the negative logarithm multiplied by the factor 2.5, so that a difference of 5 magnitudes corresponds to a luminosity ratio of 100 [10]. As this scale is highly empirical and affixed to photomultiplier measurements on spectrally different reference stars, there is a concern that the different measuring conditions for m_{vis} and cd/m^2 might lead to decalibration [18]. To check for this, the LS-110 luminance meter was used to give readings from (almost) pointlike light sources like brighter planets or first magnitude stars, after which the logarithm of the air-mass-corrected readings Y were plotted over their published visual magnitudes [14]. The resulting graph (Fig. 1) is proof of a very good linear relationship between B and $\log Y$, coinciding with a fitted line of unit slope within measurement errors, so we do not expect any major differences of the astronomically and photometrically scaled results. Because of its $(1/3)°$ measuring spot, the instrument neglects about 60% of the Moon's integral luminous flux; so to compare readings of the Moon with the point-source magnitudes in Fig. 1, the former must be corrected upward by approximately 1 magnitude. Nevertheless, the LS-110 lightmeter can determine the Moon's brightness down to about $+0\,\mathrm{m_{vis}}$, covering a dynamic brightness range of approximately $13\,\mathrm{m_{vis}}$ (a factor of 150,000), which is sufficient for recording the eclipses reported in this paper.

For the typical full Moon with an estimated luminance 3670 cd/m^2 as discussed in section 2, the

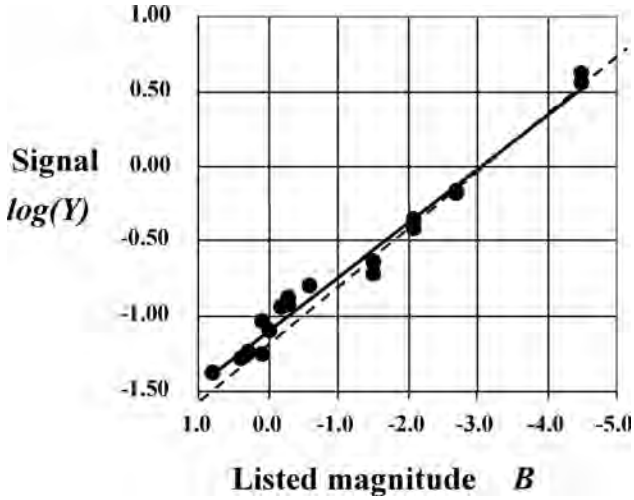

Fig. 1. Log-linearity of the LS-110 luminance photometer's scale for selected stars and planets (solid line, linear regression model; dashed line, same with unit brightness slope). Because these objects are essentially pointlike, the instrument's readings Y are not luminances, but proportional to their luminous intensities.

astronomical literature gives the brightness magnitude $-12.73\,\mathrm{m_{vis}}$ [10]:

$$B_{m,0} = -12.73\,\mathrm{m_{vis}} \triangleq L_{m,0} = 3670\,\mathrm{cd/m^2}. \quad (7)$$

However, this correspondence is correct only when the Moon is at the mean distance, because, whereas the Moon's luminance is invariant of distance, its luminosity increases with the square of the ratio of actual radius ρ_m to the mean radius $\rho_{m,0} = 15.54'$[10]. The actual visual magnitudes $B_{m,a}$ during an eclipse have to be calculated from the measured (and air-mass-corrected) luminance values $L_{m,a}$ by adding the logarithm of this geometrical factor:

$$B_{m,a} = B_{m,0} - 2.5 \times \log\left(\frac{L_{m,a}}{L_{m,0}}\right) - 5 \times \log\left(\frac{\rho_m}{\rho_{m,0}}\right). \quad (8)$$

To be able to compare the eclipse brightness of the Moon for all seasons of the year, the varying distance of the Sun must be taken care of, which according to Eq. (3) in Section 2 makes any actual luminance of the Moon vary with respect to its standardized value L_{std} at unit solar distance according to

$$\frac{L_{m,a}}{L_{m,\mathrm{std}}} = \left(\frac{d}{d_a}\right)^2 \approx \frac{1}{r_s^2}, \quad (9)$$

where and d and d_a are mean and actual Sun–Moon distances and r_s is the actual solar distance given in astronomical units. Therefore, fully standardized eclipse brightness magnitudes $B_{m,\mathrm{std}}$ must be either based on the standardized luminance values $L_{m,\mathrm{std}}$ or have subtracted the Moon distance correction in Eq. (8) and are therefore given by either expression in (10):

$$B_{m,\mathrm{std}} = B_{m,0} - 2.5 \times \log\left(\frac{L_{m,\mathrm{std}}}{L_{m,0}}\right) \overset{\text{Eq. (9)}}{=} B_{m,0} - 2.5 \times \log\left(\frac{L_{m,a}}{L_{m,0}}\right) - 5 \times \log r_s. \quad (10)$$

4. Lunar Eclipse Measurements

A. Results

Table 1 lists the main parameters for the two reported total lunar eclipses [2]. Lunar eclipses are true eclipses and therefore synchronous events for a whole hemisphere of the Earth.

The diagrams in Figs. 2 and 3 contain the air-mass-corrected actual brightness magnitudes $B_{m,a}$ for the two lunar eclipses according to Eq. (8). At the start, the 1990 eclipse was hampered by haze and low altitude. This is why the first part of the respective data (the open symbols) are excluded from the quantitative fit in Section 5. During the 2007 eclipse very clear skies became cloudy just after the start of the total phase; nevertheless all the taken data points are quantitatively useful. Except for this, both curves are believed to be accurate to one or two tenths of a visual magnitude. This level of precision is hard to reach even by experienced visual observers who compare the Moon's brightness (attenuated by different methods during the partial phases) with the brighter planets or stars [19,20]. Of course, photographic [21] and photoelectric recordings of lunar eclipses [20,22,23]are proven alternatives to our method of photometry, provided that the data are also calibrated by considering the true

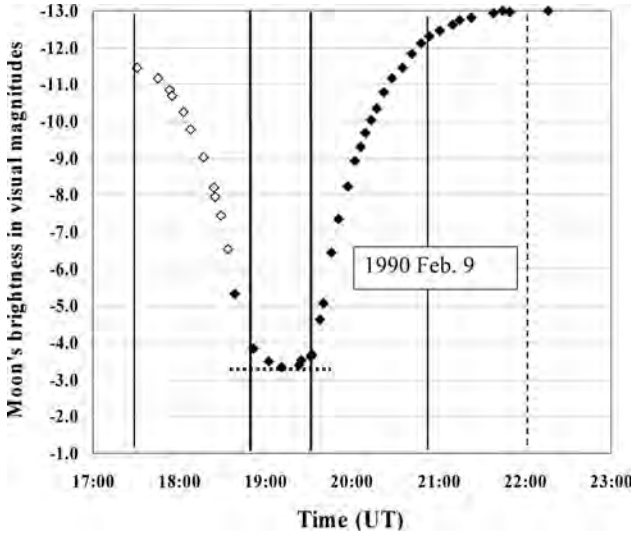

Fig. 2. Air-mass-corrected brightness magnitudes of the 9 February 1990 total lunar eclipse. Vertical lines designate the onset or end of the penumbral (dashed), partial (thin solid), and total eclipse stages (thick solid lines); the open symbols were affected by haze and therefore not used for Fig. 6.

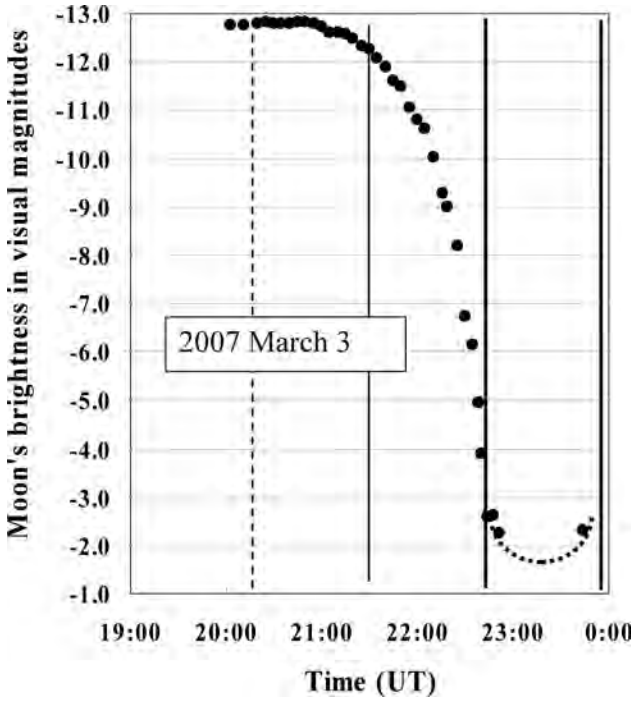

Fig. 3. Air-mass-corrected brightness magnitudes of the 3 March 2007 total lunar eclipse. The vertical lines are used in the same way as in Fig. 2. The dotted extrapolation of the light curve to the minimum brightness, missing from the measurements because of clouds, is based on a scaled rendition of Fig. 2.

lunar opposition surge, and not rather normalized indiscriminately to an assumed standard brightness near $-12.7\,m_{vis}$ for the pre-eclipse Moon [24], because this is offset by at least $-0.2\,m_{vis}$ from the true maximum lunar brightness as deduced from our data (see Table 2).

The uneclipsed Moon's brightness magnitudes in Figs. 2 and 3 show a significant difference between the two eclipses, which is explained mostly by the different lunar distances at the two events. The weakening of moonlight by the penumbra shows also precisely in our data as $(0.55 \pm 0.05)\,m_{vis}$, which translates into a linear effect of (1.66 ± 0.08) using data from the two eclipses. On the other hand, the corresponding decrease in brightness during the partial phase is different for the two events, namely $(8.7 \pm 0.3)\,m_{vis}$ for the 1990 eclipse, and $(9.6 \pm 0.3)\,m_{vis}$ for the 2007 eclipse. This deviation is not to be expected in the first place, because the umbral magnitude U (see Section 5) is at an identical value of 1.0 at the end or start of the partial phase. We believe that part of the difference has to do with lunar topography, because when comparing the trajectories for the two eclipses it is clear that the Moon's brighter southern highlands were in the outer and brighter parts of the umbra in 1990, but in the darker parts in 2007. Still, we choose not to include this information in the models of Section 5, for lack of symmetry in the data coverage of the eclipses.

Table 2 is a compilation of the maximum and minimum brightness and luminance values for the two total lunar eclipses reported here. Other than for Figs. 2 and 3, these values have been standardized to unit lunar and solar distances by Eqs. (9) and (10) as explained in Section 3. The remaining, slightly lower full Moon luminance and brightness for the 2007 eclipse is thought to be related to uncorrected, extra aerosol absorption at the onset of the 2007 lunar eclipse when a rain front had just dissipated at our location. It is well known that the scale height for aerosol extinction is much less than the barometric scale height, so data points taken at low altitudes z are very much affected [17]. Still, an unexplained difference of $0.09\,m_{vis}$ is quite an achievement with the understanding that separate luminance metering instruments were used and that the pencils of light toward the uneclipsed Moon were different by almost half a standard air mass for the two eclipses.

B. Comparison with Published Data and Predictions

To illustrate the widely varying visual estimates by contrast, we list some of the Internet published minimum light estimates for the 3 March 2007 eclipse as follows: $-2.3\,m_{vis}$ (John Bortle, Stormville, New York) and $-2.5\,m_{vis}$ (Joe Rao, New York), both from [25]; $-2\,m_{vis}$ (P. Schlyter, Stockholm, Sweden) [26]; $(-1.1 \pm 0.3)\,m_{vis}$ (four observers of REA in Brazil); and $-1.3\,m_{vis}$ (Costeira, Brazil) [27].

Our data from Table 2 exclude any values of $-2\,m_{vis}$ or brighter for the bottom level of intensity, because the 3 March 2007 eclipse was already as dark at the beginning and end of the totality. Rather, our extrapolated standardized data (these are $-0.05\,m_{vis}$ brighter than the actual data shown in Fig. 3) hint at a minimum brightness magnitude of

Table 2. Photometric Results for Two Total Lunar Eclipses

Photometric Quantity	Abbreviated [a]	Units	9 Feb. 1990	3 March 2007
Full Moon luminance	$L_{m.\,max}$	cd/m^2	4450 ± 150	(4100 ± 150) [b]
Minimum luminance	$L_{m.\,min}$	cd/m^2	0.63 ± 0.03	0.14 ± 0.04 [c]
Linear dynamic range	$L_{m.\,max}/L_{m,min}$		7100	29000
Full Moon brightness	$B_{m.\,max}$	m_{vis}	-12.94 ± 0.05	-12.85 ± 0.05 [b]
Minimum brightness	$B_{m.\,max}$	m_{vis}	-3.32 ± 0.04	-1.7 ± 0.3 [c]
Magnitude drop	$B_{m.\,min} - B_{m,max}$	m_{vis}	9.6 ± 0.1	11.15 ± 0.35

[a] Despite the missing subscripts "std," all tabulated quantities have been standardized according to Eqs. (9) and (10).
[b] Probably underestimated because of extra aerosol absorption toward the low-altitude pre-eclipse Moon.
[c] These values were extrapolated because of clouds at mid-totality, hence the larger relative error margins.

$(-1.7 \pm 0.3)\,m_{vis}$. This is only marginally consistent with the visual estimates listed above, but coincides with a prediction $(-1.5\,m_{vis})$ based on a list of lunar eclipse brightness simulations by A. Mallama [28], seemingly based on Link's empirical model for the radial intensity gradient of the Earth's umbra [3]. The prediction of this work for the 1990 eclipse is $-3.0\,m_{vis}$ [28], slightly underestimating our high-precision value $(-3.32 \pm 0.04)\,m_{vis}$. A more heuristic approach to predict the minimum brightness of lunar eclipses is to fit the minimum brightness magnitudes (mostly from visual estimates) for 24 "normal" eclipses (i.e., not affected by stratospheric aerosol from volcanoes) between 1956 and 2001 to the maximum eclipse magnitude U_{max} (see Section 5) in a linear regression model [24]:

$$B_m = -7.34 + 4.29 \times U_{max}. \quad (11)$$

Expression (11), however, describes our measurements only quite generally, predicting $-2.7\,m_{vis}$ for the 1990 eclipse and $-2.0\,m_{vis}$ for the 2007 eclipse.

5. Eclipse Light Curve Modeling

A. Earth Shadow Model

The theoretical approach for modeling light curves during lunar eclipses is based on a solar eclipse model, reported elsewhere [29]. Although the geometry and physics of lunar eclipses is quite different from solar eclipses, it is easily possible to extend the circular geometry of the solar eclipse model to also predict the luminosity of the Moon undergoing an eclipse.

During a lunar eclipse, the Moon crosses the Earth's umbra, where it is exposed to the remaining solar illuminance E_s after the Sun's light has been refracted and attenuated by the Earth's atmosphere. Including a diffuse reflection with a mean value for the lunar albedo C, the Moon thus attains the emittance M_m, which is proportional to its luminance according to Eq. (3). Due to the variations of solar illumination within the umbra, one has to add up the differing contributions over the lunar surface, facing the Earth, thus determining the Moon's relative luminous intensity I, or, after taking 2.5 times the logarithm of I and adjusting this to the full Moon's value, its brightness magnitude.

The main input parameter of the model for the Moon's luminance is the radiance distribution within the Earth's shadow. It can be calculated after considering refraction by the Earth's atmosphere, the attenuation of solar radiation within the Earth's atmosphere due to molecular scattering, ozone absorption, and aerosol scattering, as well as the attenuation by the cloud cover and topography of the Earth. The specific size of the effects obviously varies as a function of aerosol content and cloud cover of the atmosphere. Figure 4 gives an example using reasonable assumptions for the latter (see figure caption, for details; cf. [30]). It is evident that due to the angular variation of the residual solar radiance, there will be a strong gradient of radiance across the eclipsed Moon's disk.

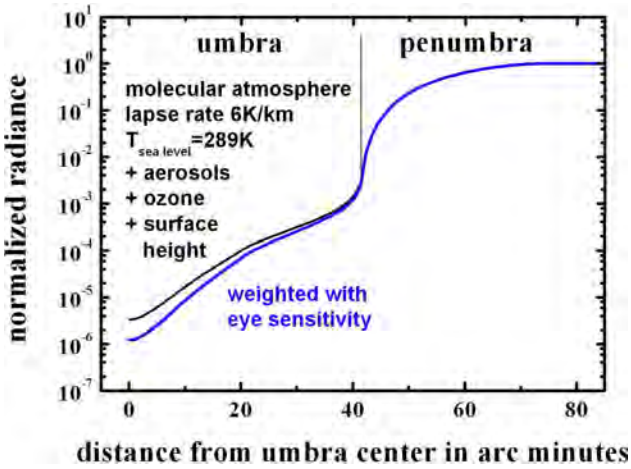

Fig. 4. (Color online) Typical normalized radiance (upper curve) distribution $H(x)$ within umbra and penumbra as a function of relative angular position. The following parameters apply: ozone concentrations 300 Dobson units, aerosols with an average optical depth such that they scatter or absorb the same amount of light as does the molecular atmosphere, and cloud cover as well as topography are modeled by a geometrical barrier, corresponding to 1 km surface height (for details see [30]). The lower curve represents $S(x)$, i.e., the curve $H(x)$ weighted by the eye sensitivity, accounting for typical brightness sensation of human observers; i.e., $S(x)$ is suitable for estimating luminance.

The radiance distribution within the umbra is modeled as a central disk (center of umbra) of normalized radiance H_1, surrounded by a number of rings with normalized radiances H_1, H_2, H_3, H_4 etc. The normalized radiance has its maximum value $H_{out} = 1.0$ just outside of the penumbra. The principle of the model is illustrated with a model of central disk plus four rings (Fig. 5). An extension to more rings is straightforward, and all subsequent model calculations were done with a model of at least 20 and as many as 40 rings, to truly represent the large variation of the radiance even with respect to the size of the Moon.

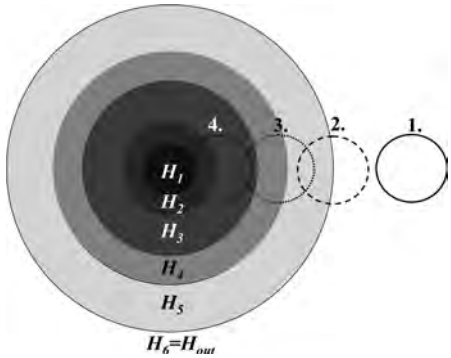

Fig. 5. Simplified geometry: the relative luminance within the umbra and penumbra is modeled by a disk plus a number of rings (here four) of certain width, each characterized by a constant normalized luminance (stepwise gray scale) of residual solar illumination. Four different positions of the Moon during the eclipse are shown (for details see text).

Figure 5 depicts several locations of the Moon with regard to the shadow. In position 1, the Moon is illuminated by the full sunlight, i.e., it is completely outside the shadow region. In position 2, part of the Moon is still outside of the penumbra, but part of it is within the outer ring. The portion on the outside reflects the unobscured fraction of the Moon's solid angle $(1 - p_i)$; the inside portion is the obscured fraction p_i of the Moon's solid angle, which is overlapping either the central disk (for $i = 1$) or an assumed disk of outer angular radius ρ_i for the ring zones ($i \geq 2$). In location 3, the Moon's disk is in three different rings of the shadow; in location 4 it is the central disk and two adjacent inner rings. The degree of overlap of the Moon's disk of angular radius $\rho_{m(oon)}$ and the shadow disks with angular radii ρ_i can be taken from the analytical calculation in the related simulation of solar eclipses [29].

B. Relative Intensity Summation and Adjustment

The idea behind the presented model for the eclipsed Moon's luminosity is simple. Assuming that the albedo of the Moon is independent of wavelength in the visible spectral range and constant over the lunar disk within this model, the total radiant intensity of the Moon follows from adding up all radiance contributions H_i falling on the Moon's disk within the various ring segments. By prior weighting of the differing radiance spectra for the various parts within the umbra and penumbra with the standard eye sensitivity curve $V(\lambda)$ [5], the transition from radiant intensity to luminous intensity is performed, which is necessary to compare the model with the measurements in Section 4. To simplify the procedure, the resulting weighted radiance distribution $S(x)$ has been calculated once and is shown as the lower curve in Fig. 4.

If p_1, p_2, p_3, etc. designate the fractional obscuration of the Moon's apparent disk by the central disk of angular radius ρ_1 and normalized weighted radiance S_1, and by the disks with angular radii ρ_2, ρ_3 (referring to the outer radii of the rings) and normalized weighted radiances S_2, S_3, etc., the normalized brightness I_{norm} of the Moon in the disk-plus-four-ring-model can then be expressed as

$$I_{\text{norm}} = p_1 S_1 + (p_2 - p_1) S_2 + (p_3 - p_2) S_3 + (p_4 - p_3) S_4 + (p_5 - p_4) S_5 + (1 - p_6) S_6. \tag{12}$$

This can be simplified in a summation scheme

$$I_{\text{norm}} = \sum_{n=0}^{5} (p_{n+1} - p_n) S_{n+1}. \tag{13}$$

By comparing (13) to (12), it becomes apparent that the value $p_0 = 0$ is introduced to account for the instance that the innermost zone of the model umbra is not a ring, but a central disk, and that the value $p_6 = 1$ correctly includes the contribution from the unrestricted zone of maximum radiance outside of the penumbra. This formula is easily generalized to an inner disk plus an arbitrary number N of rings to

$$I_{\text{norm}} = \sum_{n=0}^{N+1} (p_{n+1} - p_n) S_{n+1}. \tag{14}$$

Here, S_1 refers to the inner disk's relative luminance, S_2 to S_{N+1}, to the respective luminances in the N rings, whereas $S_{N+2} = 1$ is the relative luminance outside of the shadow, which is adjusted to unity.

Hence, the problem consists of calculating the Moon's fractionally obscured parts p_i $[i = 1 \ldots (N + 1)]$ with respect to the various radii of the modeled Earth umbra's central disk and rings. Of course, the relevant angular dimensions must be taken from databases for any lunar eclipse of interest [2]. The only additional input parameter is the weighted radiance distribution $H(x)$ (or luminance $S(x)$) within the umbra, which has been calculated in a radiative transport model for the Earth's atmosphere [30]. Therefore, after integrating all contributions from the overlapping zones, this model can be regarded as a first principles calculation of the Moon´s relative luminous intensity I_{norm} curve during an eclipse.

In a slightly more realistic model, the opposition effect of the Moon is taken into account, i.e., the fact that the lunar albedo increases steeply for small phase angles near the full Moon phase. The maximum luminosity of the Moon, which is used to normalize the theory, occurs when the Moon is just outside of the penumbra, which for the eclipse of 1990 corresponds to a phase angle of 1.5°. When the Moon just starts to contact the umbra, the phase angle is about 0.95°. Under these conditions the lunar albedo is higher by about 7%, as determined by space-based observations [9]. In the total phase of an eclipse, the effective phase angle never becomes much smaller than this, because the Moon's illumination then comes from the luminous ring of the Earth's atmosphere, which in a perfectly central eclipse subtends a circle with radius of about 0.95°. Using these relative albedo values within the model, i.e., multiplying the various ring contributions by albedo correction factors, lead to slightly larger theoretical signals than without the opposition effect.

C. Generalized Eclipse Light Curves

The model results will be presented in terms of generalized light curves. The reason is that time-line graphs of lunar eclipse brightness like those in Figs. 2 and 3 only indirectly hint at the eclipse depth. A more general way of drawing these light curves plots the Moon's brightness or luminance versus the varying umbral magnitude U of the eclipse. This quantity is obtained by dividing the angular penetration depth of the advancing perimeter of the Moon by its apparent diameter, so that any value of U equal to or greater than 1 designates a total eclipse. When

U surpasses approximately 1.33 the Moon's disk is starting to overlap the umbra's center; these eclipses are sometimes called central. Both eclipses from Table 1 were not central, probing the outer parts of the Earth's umbra only. The changing value of U during an eclipse can be calculated from one of the formulas, Eq. (15), where ρ_U and ρ_m are the angular radii of the umbra and Moon, respectively. The phase angle φ was discussed in Section 2 and is obtained by a Flash application on the internet with the accuracy of a hundredth of a degree [31]:

$$U = \frac{\rho_U - (\varphi - \rho_m)}{2\rho_m} = \frac{1}{2}\left(1 + \frac{\rho_U - \varphi}{\rho_m}\right). \qquad (15)$$

It should be noted that by this definition negative values of U can occur, representing eclipse phases when the Moon is completely outside of the umbra. Within the fit model described in Subsection 5.A, the eclipse magnitude U follows directly from the input geometrical quantities.

Figure 6 replots the observed data from the two eclipses in Figs. 2 and 3 over the respective umbral eclipse magnitudes U. Obviously, the geometrical differences of the two eclipses, i.e., the different angular sizes for the Moon and umbra, cancel out well in this plot. Figure 6 also contains a model fit for the two lunar eclipses presented in here, including the albedo correction due to the lunar phase angle effect as discussed in Subsection 5.B. In this generalized plot, the differences for the two separate eclipse fits, based on the different geometries, are also so small (below the linewidth), that they are represented by a single model curve. Its shape is defined by the model geometry, whereas the Moon's absolute brightness outside of the penumbra was chosen as the mean value of the two eclipses, namely, $-12.89\,\mathrm{m_{vis}}$ (cf. Table 2). Obviously, the comparison between observations and the model is very good, keeping in mind that the only input parameter besides geometry is the luminance distribution within the umbra.

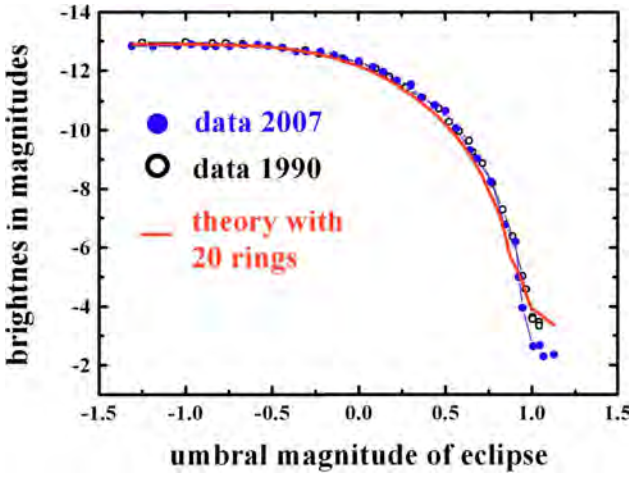

Fig. 6. (Color online) Standardized brightness magnitudes $B_{m,\mathrm{std}}$ for two total lunar eclipses (open circles, 9 February 1990 eclipse; solid dots, 3 March 2007 eclipse) compared with the results of a model calculation (solid curve).

There are a few minor exceptions to this. Between 0.0 and 0.8 umbral magnitude, theory underestimates the visual brightness approximately by $(0.2\text{–}0.3)\,\mathrm{m_{vis}}$. In the total eclipse phases $(U > 1)$ the situation is reversed. The deviations are reduced by about $0.1\,\mathrm{m_{vis}}$ if an individual fit is used for the 1990 eclipse, whereas an individual fit for the 2007 eclipse shows somewhat larger deviations. This different behavior of the two eclipses is due to the small intrinsic difference of their light curves as evidenced in Fig. 6, whereas the theoretical light curves have more or less the same shape, representing the 1990 eclipse data slightly better.

The small but apparent deviations between theory and observations for $U < 1$ are probably due to the simplicity of the radially symmetric model. We suppose that two factors may have contributed. First, the lunar albedo depends quite noticeably on the specific region on the Moon (e.g., when comparing the visible northern and southern lunar quarter spheres). Thus, for different trajectories of the Moon within the umbra, the relative contributions of high or low albedo regions may vary, which can lead to asymmetries in the observed luminance. Still, this factor does not fully explain the strong effects, occasionally showing in anomalously asymmetric lunar eclipse light curves [32]. These are pointing to true asymmetries of the luminance distribution within the umbra, due to nonsymmetric attenuation of light along the eclipse terminator.

Finally, the deviations in the eclipse brightness for $U > 1$, i.e. during the total eclipse phase, point to underestimated attenuation within deeper regions of the umbra, possibly due to the simple model for the radiance distribution within the Earth shadow. Only further investigations, which nowadays could be using satellite data for the realistic distributions of ozone, aerosols, clouds, and topography as a better set of input data for the umbra model, are expected to explain the asymmetries and deviations of the radiance and luminance distribution within the real Earth's umbra.

6. Discussion

There is a body of telescopic photoelectric measurements for lunar eclipses, mostly performed on miniscule parts of the lunar disk [33]. This is good for probing the relative radial intensity gradient of the umbra, but at the price of losing absolute calibration and sometimes also precision. Using modern CCD imaging detectors for quantitative evaluations has allowed full disk or simultaneous multispot photometry of lunar eclipses and could possibly be the method of choice for future work [34]. For the lunar eclipse of 3 March 2007, spatially resolved data in two NIR wavelength bands have been used to reintegrate the stratospheric aerosol and tropospheric water content near the twilight terminators on Earth during the totality [35]. Another interesting result of

this work shows the IR brightness of the umbra to flatten out at only about 0.001 of the full Moon level [35], whereas the visual dynamic range as determined in Fig. 3 and reported in Table 2 is almost 30,000.

The minimum level of intensity in lunar eclipses is important, because it is influenced not just by the specific eclipse depth or magnitude but also by several factors related to the amount of refraction and attenuation (extinction) in the Earth's atmosphere. Any sunlight that reaches a totally eclipsed Moon has been diverted by the lensing effect of the atmosphere along very long pathways, thus sensibly taking in any scattering and absorbing components [3,30,36]. Stratospheric dust from massive volcanic events is an especially strong factor for diminishing the Moon's brightness during total eclipses [37–39].

In this work we presented a method for obtaining accurately calibrated series of brightness measurements for total lunar eclipses to improve the aforementioned correlations. An umbral shadow simulation based on a first principle radiative transfer model of the Earth's atmosphere models the data satisfactorily. More refined approaches must take into account light curve asymmetries due to both the lunar topography and differences for the atmospheric conditions along the Earth's illuminating terminators. The inclusion of the opposition effect could be further improved by detailed ray tracing connecting the different parts of the illuminants (i.e., of the Sun and/or the atmospheric ring lens) with the correspondingly exposed areas on the lunar disk. An 11 h measurement series covering the total lunar eclipse of 28 August 2007 from a high-altitude observatory in Hawaii is currently being analyzed for these purposes [40].

The authors are much obliged to Christian Wersig (Roche Diagnostics, Mannheim, Germany) for lending the photometers used in this work, and to Dieter Kooß (Lichttechnisches Institut, University of Karlsruhe, Germany) for using a secondary luminance standard to check the instrument calibration. E. Schmidt thanks Uwe R. Ruppender of Mannheim, Germany for helping with the 1990 eclipse measurements and Yasmin A. Walter (University of Frankfurt, Germany) for providing important references. M. Vollmer thanks K.-P. Möllmann of his University for joining in a related solar eclipse measuring project and Stan Gedzelman (City College of New York, New York, USA) for valuable discussions.

References

1. B. E. Schaefer, "Lunar eclipses that changed the world," Sky Telesc. **84**, 639–642 (1992).
2. Eclipse predictions by F. Espenak, NASA/GSFC, "NASA eclipse Web site," http://eclipse.gsfc.nasa.gov/eclipse.html.
3. F. Link, "Lunar eclipses," in Z. Kopal, ed., *Physics and Astronomy of the Moon*, 1st ed. (Academic, New York 1962), pp. 161–229 [or in Z. Kopal, ed., *Advances in Astronomy and Astrophysics* (Academic, 1972), Vol. 9, pp. 67–148].
4. A. D. Ryer, *Light Measurement Handbook* (International Light, 1997).
5. L. S. Pedrotti and F. L. Pedrotti, *Optics and Vision* (Prentice Hall, 1993).
6. P. T. Landberg and V. Badescu, "The geometrical factor of spherical radiation sources," Europhys. Lett. **50**, 816 (2000).
7. D. Hahn, "Strahlung und Photometrie," in *Bergmann-Schaefer Handbuch der Experimentalphysik*, 6th ed, W. de Gruyter, ed., Vol. III of Optik (Berlin, 1974), pp. 583–637.
8. "Leuchtdichte," http://www.color-security.com/html/leuchtdichte.html.
9. B. J. Buratti, J. K. Hillier, and M. Wang, "The lunar opposition surge: observations by Clementine," Icarus **124**, 490–499 (1996).
10. C. W. Allen, *Astrophysical Quantities*, 3rd ed. (University of London Athlone Press, 1976).
11. D. L. Crawford, "Photometry: terminology and units in the lighting and astronomical sciences," Observatory **117**, 14–18 (1997).
12. J. Conrad, "Getting the right exposure when photographing the Moon," http://www.calphoto.com/moon.htm
13. "Measuring instruments,"Konica Minolta Sensing Americas, Inc., 101 Williams Drive, Ramsey, N.J. 07446, USA, http://www.konicaminolta.com/sensingusa/products/light/luminance-meter/ls100-ls110/index.htm.
14. M. Busch, "Easy Sky—your desktop planetarium," V 4.0.08, Heppenheim, Germany (June 30th, 2003), http://www.easysky.de/eng/index.htm.
15. "Key comparison—luminous intensity CCP3-K3.a1," Metrologia **42**, Technical Supplement 02001 (2005),
16. F. Kasten and A. T. Young, "Revised optical air mass tables and approximation formula," Appl. Opt. **44**, 5723–5736 (1989).
17. M. Vollmer and S. D. Gedzelman, "Colours of the Sun and Moon: the role of the optical air mass," Eur. J. Phys. **27**, 299–309 (2006).
18. A. T. Young, Department of Astronomy, San Diego State University, 5500 Campanile Drive, San Diego, Calif. 92182, USA (personal communication, 2007).
19. B. H. Granslo "Observations of the 2001 January 9 total lunar eclipse," http://www.astro.uio.no/~bgranslo/2001jan09.html
20. H. J. Schober and A. Schroll, "Photoelectric and visual observation of the total eclipse of the Moon of August 6, 1971," Icarus **20,**, 48–51 (1973).
21. J. E. Westfall, "Photographic photometry of the total lunar eclipse of September 6, 1979," Strolling Astron. **28**, 116–119 (1980).
22. R. W. Schmude, Jr., C. Davies, and W. Hallsworth, "Wideband photoelectric photometry of the Jan 20/21, 2000, total lunar eclipse," in *International Amateur-Professional Photoelectric Photometry Communication, No. 76* (IAPPP, 2000), 75–83.
23. R. W. Schmude, Jr., "Photoelectric magnitude measurements of the lunar eclipses on May 16, 2003 and Oct. 28, 2004," Ga. J. Sci. **62** 188–193 (2004).
24. H. de Carvalho Vital, "Brightness of the total lunar eclipse of May 15–16, 2003," REA/Brasil Report no. 11, http://www.geocities.com/lunissolar2003/
25. T. Flanders, "Gazing upon Earth's shadow," http://www.skyandtelescope.com/observing/home/6335642.html
26. P. Schlyter, 4 March 2007 post in Science groupsrv.com, http://www.groupsrv.com/science/about214010.html www.groupsrv.com.
27. H. de Carvalho Vital, "Total lunar eclipse of March 03, 2007, observation report and comments," http://www.geocities.com/lunissolar2003/Mar2007/Helios_Report_2007Mar03_Lunar_Eclipse.htm.
28. A. Mallama, *Eclipses, Atmospheres and Global Change* (A. Mallama, 1996), contact Anthony_Mallama@raytheon.com; see http://www.amsmeteors.org/mallama/lunarecl/mags.html

29. K. P. Möllmann and M. Vollmer, "Measurements and predictions of the illuminance during a solar eclipse," Eur. J. Phys. **27**, 1299–1314 (2006).
30. M. Vollmer and S. D. Gedzelman, "Simulating irradiance during lunar eclipses: the spherically symmetric case," Appl. Opt. **47**, H52–H61 (2008).
31. H. C. Greier, Moon*Flash* v.1.01 http://www.greier-greiner.at/hc/flash/MoonFlash/info.htm.
32. R. Gerharz, "Photometric brightness asymmetry during a lunar eclipse," Arch. Meteorol. Geophys. Biokl. Ser. A **18**, 221–226 (1969).
33. N. Sekiguchi, "Photometry of the lunar surface during lunar eclipses," Moon Planets **23**, 99–107 (1980).
34. J. Hollan (jhollan@amper.ped.muni.cz), "Photometric overview of partial lunar eclipse, Sep 7, 2006," http://amper.ped.muni.cz/light/luminance/lun_eclipse/2006/overview.htm
35. O. S. Ugolnikov and I. A. Maslov, "Altitude and latitude distribution of atmospheric aerosol and water vapor from the narrow-band lunar eclipse photometry," arXiv.org, arXiv:0706.0660 (24 April 2008); ougol@rambler.ru
36. V. G. Fesenko, "The application of lunar eclipses for surveying the optical properties of the atmosphere," Soviet Astron. AJ **14**, 195–201 (1970).
37. R. A. Keen, "Volcanic aerosols and lunar eclipses," Science **222**, 1011–1013 (1983).
38. D. Hofmann, J. Barnes, E. Dutton, T. Deshler, H. Jäger, R. Keen, and M. Osborn, "Surface-based observations of volcanic emissions to the stratosphere," in *Volcanism and the Earth's Atmosphere,* A. Robock and C. Oppenheimer, eds. (American Geophysical Union,, 2003), pp. 57–73.
39. N. Sekiguchi, "Abnormally dark lunar eclipse on December 30, 1982," Moon Planets **29**, 195–198 (1983).
40. J. E. Barnes, E. Schmidt, and Y. A. Walter, "Precision photometry of the total lunar eclipse of Aug. 28, 2007," to be submitted to Icarus.